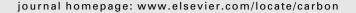


available at www.sciencedirect.com







Ordered mesoporous carbons synthesized by a modified sol-gel process for electrosorptive removal of sodium chloride

Lixia Li^{a,*}, Linda Zou^b, Huaihe Song^c, Gayle Morris^a

ARTICLE INFO

Article history:
Received 15 July 2008
Accepted 11 November 2008
Available online 20 November 2008

ABSTRACT

Capacitive deionization (CDI) represents an alternative process to remove the ions from the brackish water. In this study two series of ordered mesoporous carbons (OMCs) that demonstrated the potential use for capacitive desalination have been synthesized by a modified sol–gel process involving nickel salts. It was shown that the preferred formation of crownether type complexes between nickel ions and triblock copolymers resulted in higher BET surface area and smaller mesopores. As the electrode materials for CDI, OMC obtained by the addition of NiSO₄ · 6H₂O exhibited best electrochemical performance compared with other OMCs and a commercial activated carbon either in 0.1 M NaCl solution or in 0.0008 M NaCl solution, plus the amount of adsorbed ions measured by a flow through apparatus reached 15.9 μ mol g $^{-1}$ and the ions could be fully released into the solution. The excellent electrosorption desalination performance of OMC obtained by the addition of NiSO₄ · 6H₂O was ascribed to its high BET surface area of 1491 m 2 g $^{-1}$ and ordered mesopores of 3.7 nm. Based on these results, it is deduced that the modified sol–gel process might be a potential method of obtaining the excellent electrode materials for CDI.

 $\ensuremath{\text{@}}$ 2008 Elsevier Ltd. All rights reserved.

1. Introduction

Due to capacitive deionization (CDI)'s allure of requiring less energy and maintenance [1,2] than competitive technologies such as reverse osmosis [3] and electrodialysis [4], it is emerging as a potential technology for cleaning up the large volumes of brackish water. CDI [5,6] can be viewed as an electrochemical process that takes place in a "flow through" capacitor, where the ionic species are separated from the solution via electrostatic attractive force within the electrode/electrolyte interface under an imposed electric field. Regeneration is accomplished by electrically discharging the electrodes and yields a stream of purified water and a concentrated reject stream. On the basis of this mechanism, the electrosorption capacity strongly depends on the physical properties of electrode materials. Therefore, porous carbons

with high surface areas in the range of $400-2000~\text{m}^2~\text{g}^{-1}$, such as activated carbon [5,7] carbon nanotube [6,8] and carbon aerogel [9,10], have been proposed as suitable candidates. However, not all surface areas are available considering the existence of micropores, overlapping effect or disordered pore arrangement, which will reduce desalination efficiency.

Following the report of Ryoo et al. of CMK-1 in 1999 [11], ordered mesoporous carbons (OMCs) have rapidly attracted much attention in many applications [12–14] including as energy storage material, catalyst support and adsorbent due to their high surface areas, ordered-arranged pore structures, and narrow pore size distributions. A recent study [15] for the first time reported that OMCs could remove more amounts of ions from brackish water containing between 0.1 M and 1 M NaCl than commercial activated carbons.

^aInstitute for Sustainability and Innovation, Victoria University, Hoppers Lane, Melbourne, VIC 8001, Australia

^bCentre for Water Management and Reuse, University of South Australia, Adelaide, SA 5095, Australia

^cState Key Laboratory of Chemical Resource Engineering, Beijing University of Chemical Technology, Beijing 100029, PR China

Generally, the starting materials and the synthesis method have influence on the characteristics of OMCs. For instance, OMC derived from triblock copolymer [16] had two hystereses in N_2 sorption isotherms due to the formation of structural defects. Ji et al. [17] investigated that semi-graphitized OMC could be obtained by the reaction of post-impregnated transition salt and triblock copolymer. Liu et al. [18] developed an organic-inorganic-amphiphilic co-assembly route to fabricate OMC with nanocrystal-glass frameworks. However, it is not reported yet to prepare OMCs from inorganic-amphiphilic co-assembly in the presence of another inorganic species. In this study, OMCs were firstly prepared on the basis of the co-assembly of tetraethoxysilane (TEOS), poly(ethylene oxide)-poly(propylene oxide)-poly(ethylene oxide) triblock copolymer P123 (EO₂₀-PO₇₀-EO₂₀) and nickel salt. Their structural characterization and desalination performance were investigated by comparison with those of OMC prepared in the absence of nickel salt and a commercial activated carbon.

2. Experimental

2.1. Synthesis of ordered mesoporous carbons

For the use in the preparation, TEOS, P123, nickel sulfate hexahydrate (NiSO₄·6H₂O) and nickel nitrate hexahydrate (Ni(NO₃)₂·6H₂O) were purchased from Aldrich. The detailed process was as follows: (1) 5 g of P123 is dissolved in the solution composed of 130 ml of de-ionized water and 6.36 ml of sulphuric acid at 313 K. After the complete dissolution of P123, the nickel source was added, followed by the addition of 9.2 ml of TEOS under stirring. The mixture was aged at 313 K for 24 h, followed by further aging at 373 K for 36 h to obtain an as-synthesized composite; (2) the carbon replication was performed by the precarbonization of the as-synthesized composite at 373 K and 433 K, respectively, the carbonization at 1223 K for 6 h under N2 flow and final removal of silica and nickel. The products prepared by the addition of NiSO₄ · 6H₂O and Ni(NO₃)₂ · 6H₂O are denoted as OMC-S and OMC-N, respectively, where S and N indicate the kind of nickel salt used. To investigate the effect of nickel source on the resultant carbon material, an ordered mesoporous carbon without the use of nickel salt was prepared by fixing the mass ratio of other raw materials, and is here denoted as OMC-W, where W represents the absence of nickel salt.

2.2. Characterization of ordered mesoporous carbons

The carbon materials were characterized by small-angle X-ray scattering (SAXS), transmission electron microscopy (TEM) and N_2 adsorption–desorption measurements. SAXS patterns were collected on a Bruker Nanostar using Cu K α radiation at 40 kV and 40 mA. Each sample was scanned over the q range of 0.1–3.0 nm $^{-1}$. TEM measurement was conducted using Hitachi H-800 electron microscope. Nitrogen adsorption–desorption isotherms were performed with a Micromeritics Tristar 3000 analyzer at 77 K. Before measurements, the samples were degassed in a vacuum at 473 K for overnight. The pore size distribution was calculated by the BJH (Barrett–Joyner–Halenda) method from the desorption

branch. $D_{\rm me}$ represents the pore diameter corresponding to the peak position of pore size distribution curve. The specific surface area ($S_{\rm BET}$) was calculated from the adsorption data in the relative pressure interval from 0.04 to 0.2 using the Brunauer–Emmett–Teller (BET) method. The total pore volume ($V_{\rm t}$) was estimated from the amount adsorbed at a relative pressure of 0.98. The micropore volume ($V_{\rm mi}$) and micropore surface area ($S_{\rm mi}$) were calculated by the t-plot method. The nickel loading of the silica/carbon/nickel composite was measured by flame atomic absorption on a GBC 906AA spectrometer. Typically, an air–acetylene flame was used and the used analysis method was standard addition.

2.3. Assembly and measurement of the electrodes

The mechanism and performance of electrosorption desalination were tested by cyclic voltammetry (CV). Cyclic voltammetric measurements were performed by an Autolab/PGSTAT100 potentiostat (Eco Chemie, the Netherlands) with a conventional three-electrode cell. The working electrodes were prepared by pressing a mixture of carbon (78 wt.%), graphite (20 wt.%) and polytetrafluoroethylene (PTFE) (2 wt.%) to the graphite sheet served as a current collector. The electrodes had a surface area of 100 mm² and thickness of 0.4 mm, and the mass load was 10 mg cm². Platinum and Ag/AgCl electrodes were used as the counter and reference electrodes, respectively. The electrolytes were NaCl solutions with two concentrations, namely 0.1 M and 0.0008 M. The capacitances were calculated from CV curves using the following formula:

$$C = (q_a + |q_c|)/\Delta V \tag{1}$$

where C is the capacitance, q_a and q_c are the anodic and cathodic voltammetric charges on positive and negative sweeps, respectively, and ΔV is the potential range. No gas bubbles were observed during the measurements, so the gas sparging was not performed. The noise levels were not significant at used NaCl concentrations.

2.4. Removal of NaCl

Adsorption efficiencies of ions on electrodes were measured using a flow through apparatus including an electrosorption unit cell shown in Fig. 1. NaCl was removed by applying a direct voltage of 0.8 V between the electrodes. By removing the voltage the adsorbed ions came out to achieve the regeneration of electrodes. In each experiment, the NaCl solution was continuously pumped from a peristaltic pump into the unit cell and the effluent was returned to the cell. Wherein the solution temperature was kept at 298 K, a flow rate of around 20 ml min⁻¹ was maintained, and a total solution volume of 100 ml and an electrode mass of 1.2 g were applied. The concentration changes of NaCl solution were continuously monitored and measured at the outlet of the unit cell using a conductivity metre. NaCl adsorption capacity was calculated according to

$$M = (P_0 - P)V/m \tag{2}$$

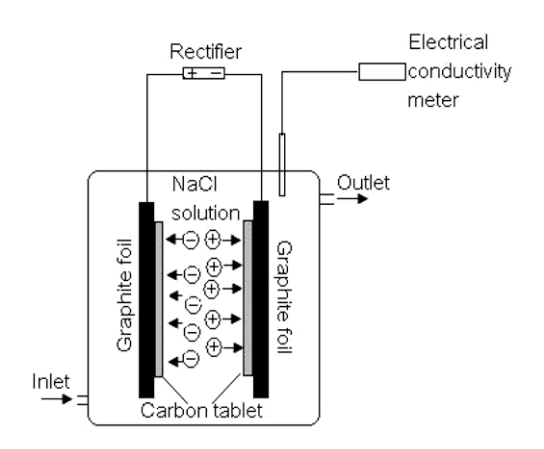


Fig. 1 - Schematic of the electrosorption unit cell.

where P_0 is the starting NaCl concentration, P is the final NaCl concentration, V is the volume of the NaCl solution, and m is the mass of active component in the working electrode.

3. Results and discussion

3.1. Characterization of ordered mesoporous carbons

It is well documented [19,20] that for co-assembly of block copolymer, metal ion and silica species in acidic conditions, transition metal ions such as Ni^{2+} and Cu^{2+} firstly form crown-ether type complexes with the alkylene oxide segments of block copolymers by weak coordination bonds, where the metal species preferentially associate with the hydrophilic PEO moieties because of their different binding affinities for PEO and PPO. Subsequently the forming complexes assemble with the silica species in the same way as the assembly of mesostructured silica/copolymer composites. Finally the ordered mesostructured silica/copolymer/metal composites will be formed as silica species cross-link and polymerize. This synthesis pathway is denoted as $N^0[(M^{n+}+H^+)X^-]I^+$, where N^0 is a non-ionic surfactant (amphi-

philic block copolymer), M^{n+} is the metal ion, HX is the acid, and I^+ is the inorganic reagent.

Fig. 2a displays the N₂ adsorption-desorption isotherms of the resultant OMCs. It is clearly observed that all the isotherms are the shape of irreversible type IV as defined by IU-PAC [21], which is characteristic of mesoporous solids. Basically the sharpness of the capillary condensation steps indicates the uniformity of mesopore size distribution [22]. As can be seen from the isotherms, the steps appear in the wide P/Po range of 0.4-0.9, indicating that their mesopores are not perfectly uniform [23], especially for OMC-W (see Fig. 2b). On the other hand, a visible increase of adsorption amount at $P/P_0 > 0.9$ could be resulted from the existence of interparticle pores. It is further deduced from Fig. 2b that the mesopore sizes of OMC-S and OMC-N prepared by the addition of nickel salt are slightly smaller than those of OMC-W prepared in the absence of nickel salt, centred at 3.7, 3.3 and 4.0 nm, respectively, which well matches with the reported results in the other literatures [24,25], i.e. the addition of metal ions will lead to mesoporous silica materials with reduced pore wall and in turn the carbon replicas with reduced pore size. Compared with OMC-N, the mesopore size of OMC-S is a bit larger due to the different amounts of deposited Ni in silica/carbon/metal composites (5.9 wt.% for OMC-N and 4.1 wt.% for OMC-S). Table 1 summarizes the textural characteristics of these OMC materials. The physical properties of OMC-S and OMC-N prepared by the addition of nickel salt are comparable, such as their BET surface areas reach $1491 \text{ m}^2 \text{ g}^{-1}$ and $1594 \text{ m}^2 \text{ g}^{-1}$, respectively, while OMC-W prepared in the absence of nickel salt has a low BET surface area and a low total pore volume, $950 \text{ m}^2 \text{ g}^{-1}$ and $1.102 \text{ cm}^3 \text{ g}^{-1}$, respectively.

The information about the pore arrangement of OMCs can be obtained by SAXS and TEM. Their SAXS patterns are shown in Fig. 3. A strong and narrow peak is observed at the q value of 0.79 nm $^{-1}$ for OMC-W prepared in the absence of metal salt. Although higher order peaks can not be clearly discerned, it is still deduced that its pores are arranged according to P6mm hexagonal structure. In comparison with OMC-W, the SAXS pattern of OMC-S prepared by the addition of NiSO₄ · 6H₂O shows a similar reflection at the q value of

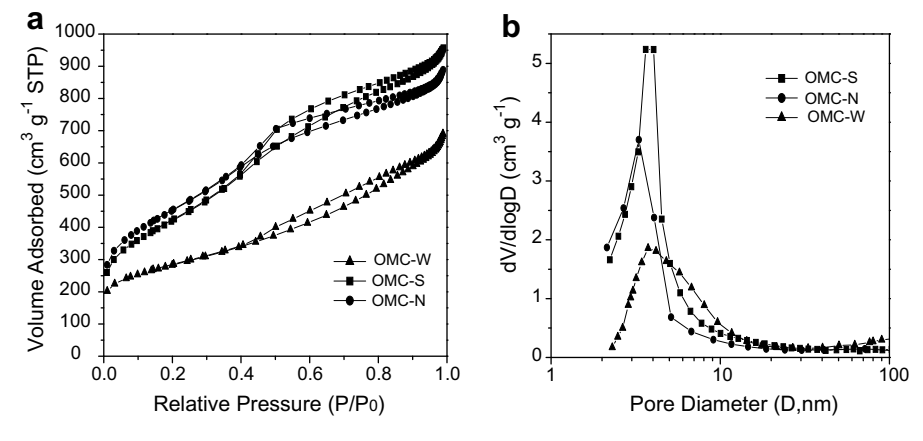


Fig. 2 - Nitrogen sorption isotherms (a) and pore size distributions (b) for these OMCs.

| Table 1 – The textural characteristics of OMCs and a commercial activated carbon. | | | | | |
|---|------------------------|-----------------------|--|-----------------------------------|----------------------|
| Sample | $S_{BET} (m^2 g^{-1})$ | $S_{mi} (m^2 g^{-1})$ | $V_{\rm t}$ (cm ³ g ⁻¹) | $V_{\rm mi}$ (cm 3 g $^{-1}$) | D _{me} (nm) |
| OMC-S | 1491 | 206 | 1.589 | 0.202 | 3.7 |
| OMC-N | 1594 | 277 | 1.453 | 0.207 | 3.3 |
| OMC-W | 950 | 298 | 1.102 | 0.238 | 4.0 |
| Activated carbon | 845 | 579 | 0.605 | 0.247 | |

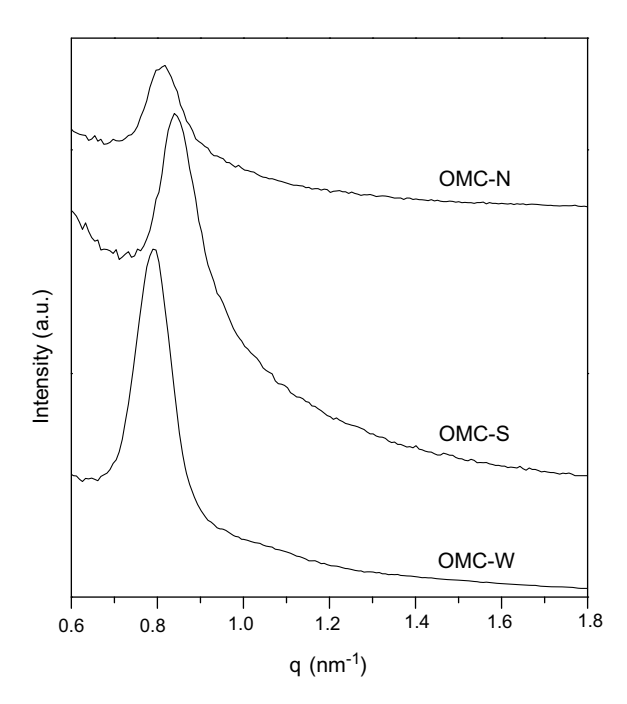


Fig. 3 - SAXS patterns of these OMCs.

 $0.83~\text{nm}^{-1}$, whereas only a broad peak with low intensity appears in the case of OMC-N prepared by the addition of Ni(NO₃)₂·6H₂O, implying that the ordering of the latter on the mesoscopic scale is low. The different effect of two nickel salts on the degree of mesoscopic order should be caused from their different decomposition temperatures during the carbonization process. The TEM images showed in Fig. 4 also confirm that OMC-S with high degree of ordered porous texture is obtained after the addition of NiSO₄·6H₂O into the synthesis.

3.2. Electrochemical characterization of ordered mesoporous carbons

Previous studies [15,26] have demonstrated that the electrosorption capacity of the porous carbon electrode is mainly affected by electrical double-layer capacity due to the electrostatic attractive force between the ion and the electrode. The electrical double layers are formed inside the pores instead of adjacent to the electrode surface. Thus, when the pore size of the electrode is similar to the electrical double layer thickness, the electrical double layers overlap and meanwhile the resulted electrical capacities are lost [1,9]. It is known that the concentration of the electrolyte solution is one important factor to affect the electrical double layer thickness. Therefore, in this study the electrosorption desalination performance of synthesized ordered mesoporous carbons is primarily investigated in both 0.1 M and 0.0008 M NaCl solutions.

Cyclic voltammetry (CV) considered as an important method in supercapacitor has been developed to evaluate the potential possibility of materials used for capacitive deionization and meanwhile the electrochemical properties such as specific capacitance can be obtained. Granular activated carbon (AC) was brought from Calgon Carbon Corporation in UK into comparison and its pore parameters are provided in Table 1. The cyclic voltammograms of OMCs and AC swept at a sweep rate of 1 mV s⁻¹ in 0.1 M NaCl solution are shown in Fig. 5. As can be observed, all the CV curves present the typical capacitor-like characteristics with "boxlike" shape in the applied potential range of -0.2-0.8 V. This means that all charge/discharge processes are stable and highly reversible. Thus, the Na+ and Cl- ions are removed from the solution by the formed electric double layers and the electrodes can be regenerated. On the other hand, in the case of OMC-S prepared by the addition of NiSO₄ · 6H₂O both cathodic and anodic currents reach higher values than other

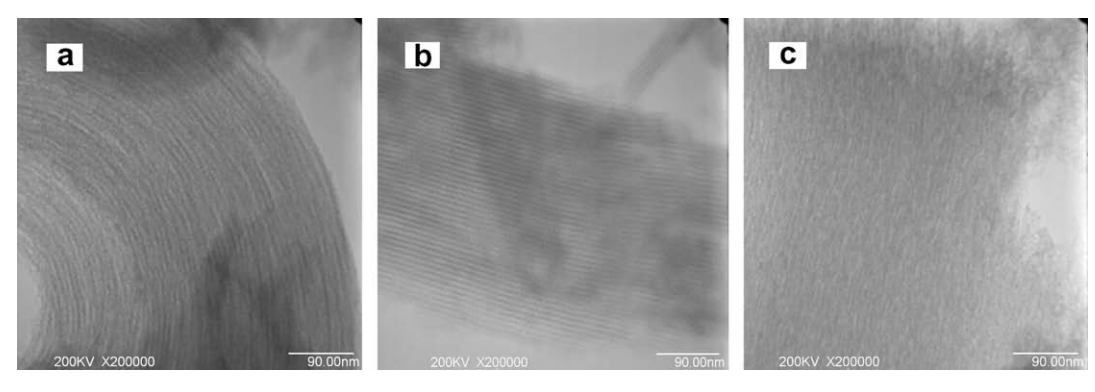


Fig. 4 - TEM images of OMC-W (a), OMC-S (b) and OMC-N (c).

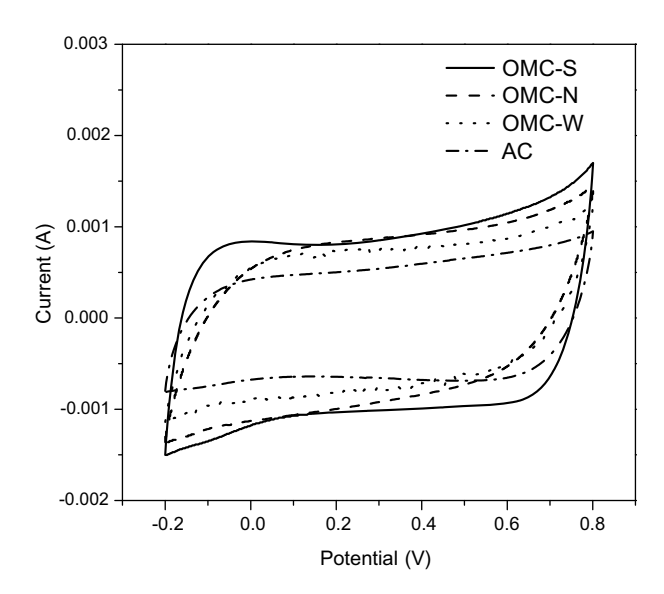


Fig. 5 – Cyclic voltammograms of OMCs and AC swept at 1 mV s^{-1} in 0.1 M NaCl solution.

three carbon materials. Its high BET surface area may play an essential role whereas the ordered mesopores of 3.7 nm are decisive for the transportation of ions. Thus the higher capacitances can be achieved for OMC-S.

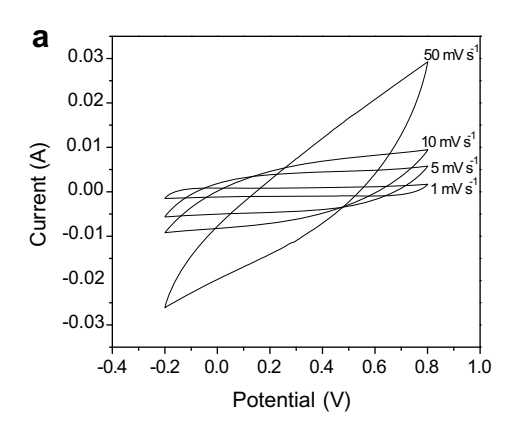
The CV curves obtained at different potential sweep rates on the capacitor with OMC-S electrode are shown in Fig. 6a. At 1 mV s⁻¹ or 5 mV s⁻¹ a rectangular shape can be observed. At 10 mV s⁻¹ the shape of rectangle is slightly distorted. At 50 mV s⁻¹ the shape is clearly distorted. Similar behaviors have been observed in OMC-N, OMC-W and even AC (see Fig. 6b). These imply that at high sweep rates the ohmic resistance for electrolyte motion in the pores has affected the double layer formation mechanism, in which the charge stored is recognized to be distributed [27]. On the other hand, the increase in the induced current with sweep rate has intensified the potential difference between the mouth and bottom of the pores, and thus a delayed current response is deduced as shown in the tilted voltammograms. This effect is the most evident for the AC-derived electrode, which will be illuminated using the following capacitance maintenance.

The calculated specific capacitances of the carbon electrodes based on Eq. (1) are plotted in Fig. 7. As can be seen, at the same sweep rate both OMC-S and OMC-N electrodes prepared by the addition of nickel salt reach higher specific capacitances than OMC-W and AC electrodes. For example, when the sweep rate of 1 mV s⁻¹ is used, OMC-S and OMC-N achieve the specific capacitances of $192 \, \mathrm{F} \, \mathrm{g}^{-1}$ and 174 F g⁻¹, respectively, whereas for OMC-W and AC the values are only 140 and 108 F g⁻¹, respectively. This implies that the desalination efficiency of carbon electrode can be improved by the addition of nickel salt into the synthesis, which is due to the increase of available pore surfaces. In addition, as mentioned above, the capacitance change with the sweep rate is also different. For instance, when the sweep rate is increased from 1 mV s^{-1} to 10 mV s^{-1} , 62% and 53% of the original capacitances are maintained for OMC-S and AC, respectively.

Since the electrical double layers with different thicknesses are formed in electrolyte solutions at different concentrations, different electrochemical properties will be resulted. The electrochemical property of each electrode was further researched in 0.0008 M NaCl solution. The CV curves recorded at a sweep rate of 1 mV s⁻¹ are shown in Fig. 8. Steady increases and decreases in current with electric potential indicate that the desalination mechanism is not varied with the concentration, i.e., the ions are electroadsorbed by the formed electrical double layers. However, for the bulk solution usually has a remarkable effect on electrochemical performance of a capacitor [1,28], at a low sweep rate of 1 mV s⁻¹ all electrodes have exhibited a capacitive behaviour with highly distorted rectangular shape. As a result of the bigger resistance, the less electrical double layers are formed than in 0.1 M NaCl solution. Furthermore, OMC-S shows the highest induced current among them, which is resulted from its high BET surface area and ordered mesopores.

3.3. CDI performance of ordered mesoporous carbons

Fig. 9 shows electrosorptive removal curves of Na $^+$ and Cl $^-$ ions from the solution on OMCs and AC. It is calculated that in 0.0008 M NaCl solution (conductivity 100 μ S cm $^{-1}$) the amounts of the adsorbed ions calculated using Eq. (2) are 15.9 μ mol g $^{-1}$ for OMC-S, 9.2 μ mol g $^{-1}$ for OMC-N,



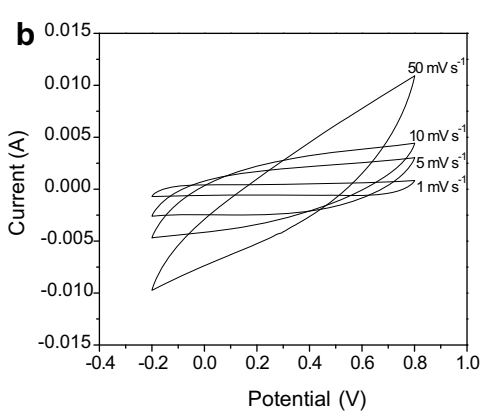


Fig. 6 - Cyclic voltammograms of OMC-S (a) and AC (b) at various sweep rates in 0.1 M NaCl solution.

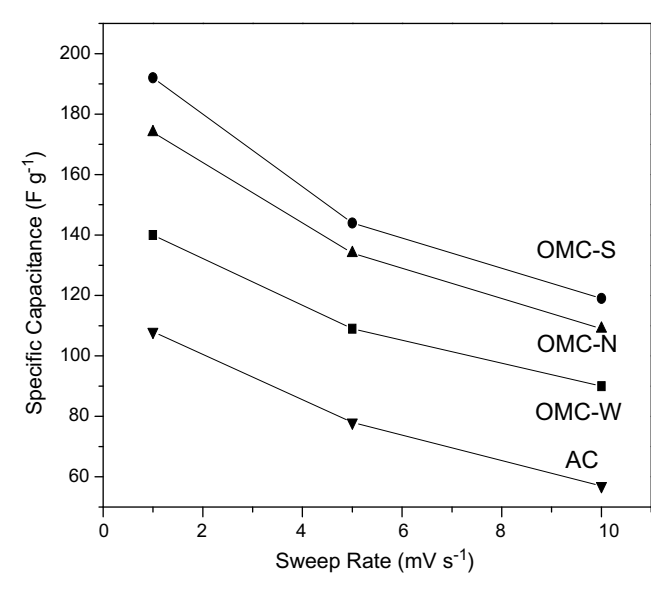


Fig. 7 – The specific capacitances of the carbon electrodes at different sweep rates in 0.1 M NaCl solution.

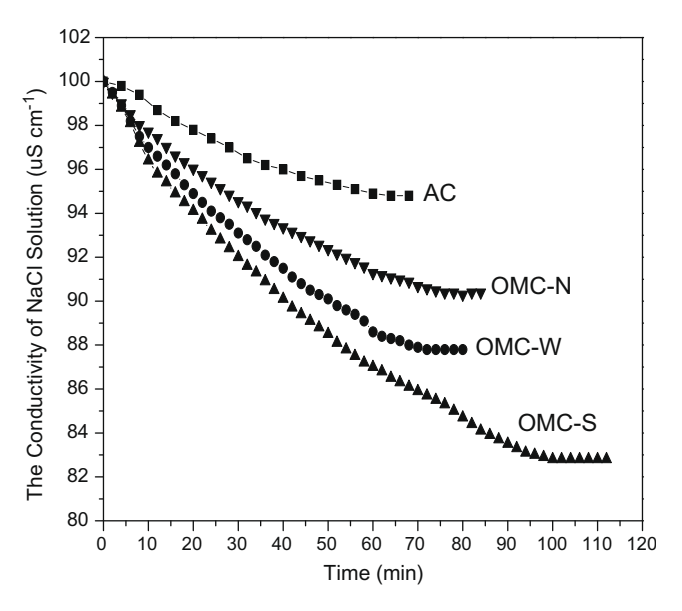


Fig. 9 – Electrosorptive removal curves of Na⁺ and Cl⁻ ions from the solution on OMCs and AC.

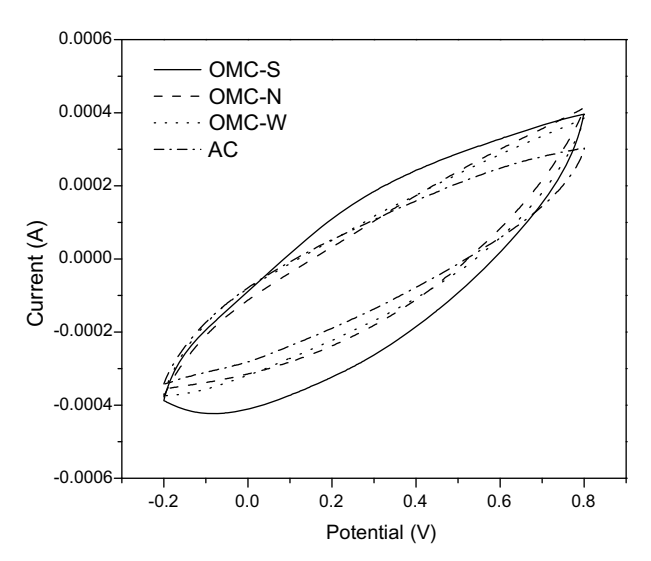


Fig. 8 – Cyclic voltammograms of OMCs and AC swept at 1 mV s^{-1} in 0.0008 M NaCl solution.

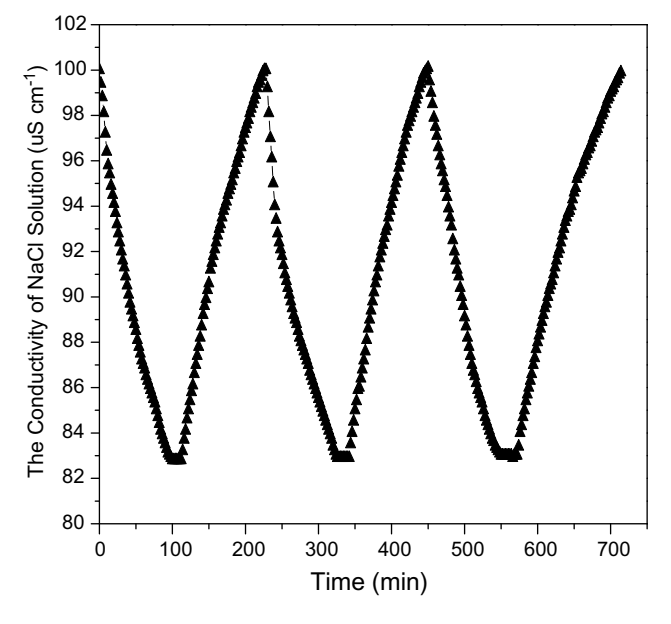


Fig. 10 - NaCl adsorption and regeneration curves of OMC-S.

 $10.3~\mu mol~g^{-1}$ for OMC-W and $4.7~\mu mol~g^{-1}$ for AC. Evidently, OMCs bring about more ions onto the surfaces of electrodes compared with AC, which is consistent with the result of cyclic voltammetry. On the other hand, it is necessary to mention that OMC-N shows somewhat lower NaCl adsorption capability than OMC-W, which seems to mean that ordered pore structure is beneficial to the transportation of ions. Additionally, regeneration of the electrodes is very important. Fig. 10 shows the characteristics of NaCl adsorption and regeneration of OMC-S. After removing the voltage the ions of OMC-S electrode are clearly released and thus the process of regeneration could be carried out.

4. Conclusions

The carbon synthesis by the addition of nickel salt into a mesoporous silica template is a route for obtaining OMCs with various structures. Here it has been demonstrated that the carbon synthesis is feasible by mesostructure-directing effect of the metal complexes formed via the interaction of metal ions with the –O– groups of the copolymers. The resultant carbons had higher BET surface areas and smaller ordered mesopores in comparison with ordered mesoporous carbons

without the use of nickel salts. In addition, their electrosorption desalination results were consistent throughout cyclic voltammetry and CDI experiment. OMC-S prepared by the addition of NiSO₄ \cdot 6H₂O exhibited maximum in the removal of NaCl due to its high BET surface area of 1491 m² g⁻¹ and ordered mesopores of 3.7 nm. The regeneration of the electrodes was confirmed.

Acknowledgements

The authors thank Victoria University for Priority Research and Innovation Project Funding, the Research Program of China Petrochemical Corporation (X504014) and the Program for New Century Excellent Talents in University of China (NCET-04-0122) for providing financial support for this research. The authors acknowledge the assistance from Dr. Xiaodong Dai in sample analysis.

REFERENCES

- Xu P, Drewes JE, Heil D, Wang G. Treatment of brackish produced water using carbon aerogel-based capacitive deionization technology. Water Res 2008;42(10–11):2605–17.
- [2] Welgemoed TJ, Schutte CF. Capacitive deionization technology™: an alternative desalination solution. Desalination 2005;183(1–3):327–40.
- [3] Basta AH, El-Saied H. Enhanced transport properties and thermal stability of agro-based RO-membrane for desalination of brackish water. J Membr Sci 2008; 310(1–2):208–18.
- [4] Banasiak LJ, Kruttschnitt TW, Schäfer AI. Desalination using electrodialysis as a function of voltage and salt concentration. Desalination 2007;205(1-3):38–46.
- [5] Ryoo M, Kim J, Seo G. Role of titania incorporated on activated carbon cloth for capacitive deionization of NaCl solution. J Colloid Interf Sci 2003;264(2):414–9.
- [6] Wang XZ, Li MG, Chen YW, Cheng RM, Huang SM, Pan LK, et al. Electrosorption of ions from aqueous solutions with carbon nanotubes and nanofibers composite film electrodes. Appl Phys Lett 2006;89(5):053127. 1–3.
- [7] Zou L, Morris G, Qi D. Using activated carbon electrode in electrosorptive deionization of brackish water. Desalination 2008;225(1–3):329–40.
- [8] Zhang D, Shi L, Fang J, Dai K. Influence of diameter of carbon nanotubes mounted in flow-through capacitors on removal of NaCl from salt water. J Mater Sci 2007;42(7):2471–5.
- [9] Yang KL, Ying TY, Yiacoumi S, Tsouris C, Vittoratos ES. Electrosorption of ions from aqueous solutions by carbon aerogel: an electrical double layer model. Langmuir 2001;17(6):1961–9.
- [10] Yang K, Yiacoumi S, Tsouris C. Electrosorption capacitance of nanostructured carbon aerogel obtained by cyclic voltammetry. J Electroanal Chem 2003;540(2):159–67.

- [11] Ryoo R, Joo SH, Jun S. Synthesis of highly ordered carbon molecular sieves via template-mediated structural transformation. J Phys Chem B 1999;103(37):7743–6.
- [12] Li L, Song H, Chen X. Pore characteristics and electrochemical performance of ordered mesoporous carbons for electric double-layer capacitors. Electrochim Acta 2006;51(26): 5715–20.
- [13] Minchev C, Huwe H, Tsoncheva T, Paneva D, Dimitrov M, Mitov I, et al. Iron oxide modified mesoporous carbons: physicochemical and catalytic study. Micropor Mesopor Mater 2005;81(1–3):333–41.
- [14] Guo Z, Zhu G, Gao B, Zhang D, Tian G, Chen Y, et al. Adsorption of vitamin B12 on ordered mesoporous carbons coated with PMMA. Carbon 2005;43(11):2344–51.
- [15] Zou L, Li L, Song H, Morris G. Using mesoporous carbon electrodes for brackish water dasalination. Water Res 2008;42(8–9):2340–8.
- [16] Kim J, Lee J, Hyeon T. Direct synthesis of uniform mesoporous carbons from the carbonization of as-synthesized silica/ triblock copolymer nanocomposites. Carbon 2004;42(12–13): 2711–9.
- [17] Ji X, Herle PS, Rho Y, Nazar LF. Carbon/MoO₂ composite based on porous semi-graphitized nanorod assemblies from in situ reaction of tri-block polymers. Chem Mater 2007;19(3):374–83.
- [18] Liu R, Ren Y, Shi Y, Zhang F, Zhang L, Tu B, et al. Controlled synthesis of ordered mesoporous C-TiO₂ nanocomposites with crystalline titania frameworks from organic-inorganicamphiphilic coassembly. Chem Mater 2008;20(3):1140-6.
- [19] James DB, Wetton RE, Brown DS. Polyether-metal salt complexes: 1. The elevation of the glass transition temperature of polyethers by metal salts. Polymer 1979;20(2):187–95.
- [20] Bailey FE, Koleske JV. Alkylene oxides and their polymers. New York: Marcel Dekker; 1990.
- [21] Kruk M, Jaroniec M. Gas adsorption characterization of ordered organic-inorganic nanocomposite materials. Chem Mater 2001;13(10):3169–83.
- [22] Kumar P, Mal N, Oumi Y, Yamana K, Sano T. Mesoporous materials prepared using coal fly ash as the silicon and aluminium source. J Mater Chem 2001;11(12):3285–90.
- [23] Fuertes AB, Nevskaia DM. Control of mesoporous structure of carbons synthesised using a mesostructured silica as template. Micropor Mesopor Mater 2003;62(3):177–90.
- [24] Kónya Z, Zhu J, Szegedi A, Kiricsi I, Alivisatos P, Somorjai GA. Synthesis and characterization of hyperbranched mesoporous silica SBA-15. Chem Commun 2003;3:314–5.
- [25] Kang T, Park Y, Yi J. Facile synthesis and characterization of ordered mesostructured nickel catalysts. J Mol Catal A: Chem 2006;244(1–2):151–9.
- [26] Vix-Guterl C, Frackowiak E, Jurewicz K, Friebe M, Parmentier J, Béguin F. Electrochemical energy storage in ordered porous carbon materials. Carbon 2005;43(6):1293–302.
- [27] Liu H, Wang K, Teng H. A simplified preparation of mesoporous carbon and the examination of the carbon accessibility for electric double layer formation. Carbon 2005;43(3):559–66.
- [28] Yoon S, Lee J, Hyeon T, Oh SM. Electric double-layer capacitor performance of a new mesoporous carbon. J Electrochem Soc 2000;147(7):2507–12.